

## Excitation Spectra of Lithium Donors in Silicon and Germanium\*

R. L. AGGARWAL, P. FISHER, V. MOURZINE,† AND A. K. RAMDAS

*Department of Physics, Purdue University, Lafayette, Indiana*

(Received 10 December 1964)

The excitation spectra of lithium in silicon and germanium have been measured. These spectra exhibit excitation lines which indicate that the excited states of lithium are similar to those of the Group-V impurities. For oxygen-free silicon and germanium, the lithium excitations observed occur at energies close to those of the Group-V transitions which originate from the upper ground states of these impurities. This indicates that the chemical splitting of the ground state of lithium in silicon and germanium may be very small. The effect of uniaxial stress on the excitation spectrum of lithium in silicon has been examined. The experimental results for lithium in oxygen-free silicon are interpreted as follows: The site symmetry of the isolated lithium is tetrahedral; the ground state is an "inverted" Group-V-like ground state, the  $1s(A_1)$  state lying  $1.8 \pm 0.1$  meV above the  $1s(E+T_1)$  state. For lithium in oxygen-containing silicon, zero-stress and uniaxial-stress measurements indicate that the ground state is Group-V-like with the  $1s(E+T_1)$  state lying  $7.7 \pm 0.1$  meV above the  $1s(A_1)$  state. The spectra of lithium in germanium and oxygen-containing silicon exhibit lines which do not fit the Group-V pattern.

### I. INTRODUCTION

LITHIUM as an impurity in the elemental semiconductors, silicon and germanium, and the III-V compounds has attracted considerable attention as a consequence of its remarkable diffusion properties<sup>1</sup> and its ability to complex with other chemical impurities which may be present in the crystals.<sup>2,3</sup> The large diffusion coefficient<sup>1</sup> has been attributed to the interstitial nature of lithium. Weiser<sup>4</sup> has considered the theory of impurity diffusion in the diamond lattice and has deduced that lithium occupies an interstitial position which is not the tetrahedral but rather the hexagonal site.

Lithium in silicon and germanium acts as a shallow donor.<sup>5,6</sup> Lithium is known to complex with dispersed oxygen in silicon and such complexes are also found to be donors.<sup>3</sup> Feher<sup>7</sup> has observed the electron spin resonance exhibited by the lithium-oxygen complex in silicon but failed to observe it for the lithium donor in floating-zone silicon. We have examined the excitation spectra exhibited at low temperatures by both lithium and lithium-oxygen complexes in silicon and by lithium

in germanium.<sup>8</sup> For the case of silicon, the spectra were also examined under uniaxial stress.<sup>8</sup> The object of the present paper is to present the results of this experimental investigation and to discuss their implications. The experimental results are given in Sec. III. In Sec. IV the excitation spectra of lithium and lithium-oxygen complexes have been compared with those of the Group-V donors and models for the ground states are discussed.

### II. EXPERIMENTAL PROCEDURE

Lithium-doped silicon samples were prepared following essentially the technique described by Pell.<sup>3</sup> Undoped floating-zone or crucible-grown silicon samples were coated with commercially available lithium dispersed in mineral oil. The oil was eliminated by heating for two hours in a helium atmosphere at 200°C. This was followed by a heat treatment at 400°C, typically for about 30 min. The sample was then removed from the furnace and the surfaces cleaned. A further heat treatment at 600°C for 2 h in a helium atmosphere was given to ensure that the lithium was homogeneously distributed. A somewhat similar procedure was followed for germanium. Lithium-doped germanium samples were also prepared from ingots grown from melts containing lithium.

A double pass Perkin-Elmer spectrometer, equipped with Bausch and Lomb plane reflection gratings and appropriate filtering systems,<sup>9</sup> was used for the measurements on silicon. A single pass Perkin-Elmer grating spectrometer with suitable filtering was used for the measurements on germanium. The optical cryostats,<sup>10</sup>

\* Work supported in part by the Advanced Research Projects Agency, Office of Naval Research and U. S. Army Research Office—Durham.

† Sponsored by the National Academy of Sciences. Present address: Physical Institute, Academy of Sciences, Moscow, USSR.

<sup>1</sup> H. Reiss and C. S. Fuller, *Semiconductors*, edited by N. B. Hannay (Reinhold Publishing Corporation, New York, 1960), Chap. VI.

<sup>2</sup> C. S. Fuller, *Semiconductors*, edited by N. B. Hannay (Reinhold Publishing Corporation, New York, 1960), Chap. V.

<sup>3</sup> E. M. Pell, *Solid State Physics in Electronics and Telecommunications*, edited by M. Désirant and J. L. Michiels (Academic Press Inc., New York, 1960), Vol. 1, p. 261.

<sup>4</sup> K. Weiser, *Phys. Rev.* **126**, 1427 (1962).

<sup>5</sup> C. S. Fuller and J. A. Ditzenberger, *Phys. Rev.* **91**, 193 (1953). See also, F. J. Morin, J. P. Maita, R. G. Shulman, and N. B. Hannay, *Phys. Rev.* **96**, 833 (1953).

<sup>6</sup> See for example, W. Kohn, *Solid State Physics*, edited by F. Seitz and D. Turnbull (Academic Press Inc., New York, 1957), Vol. 5, p. 257, Fig. 16.

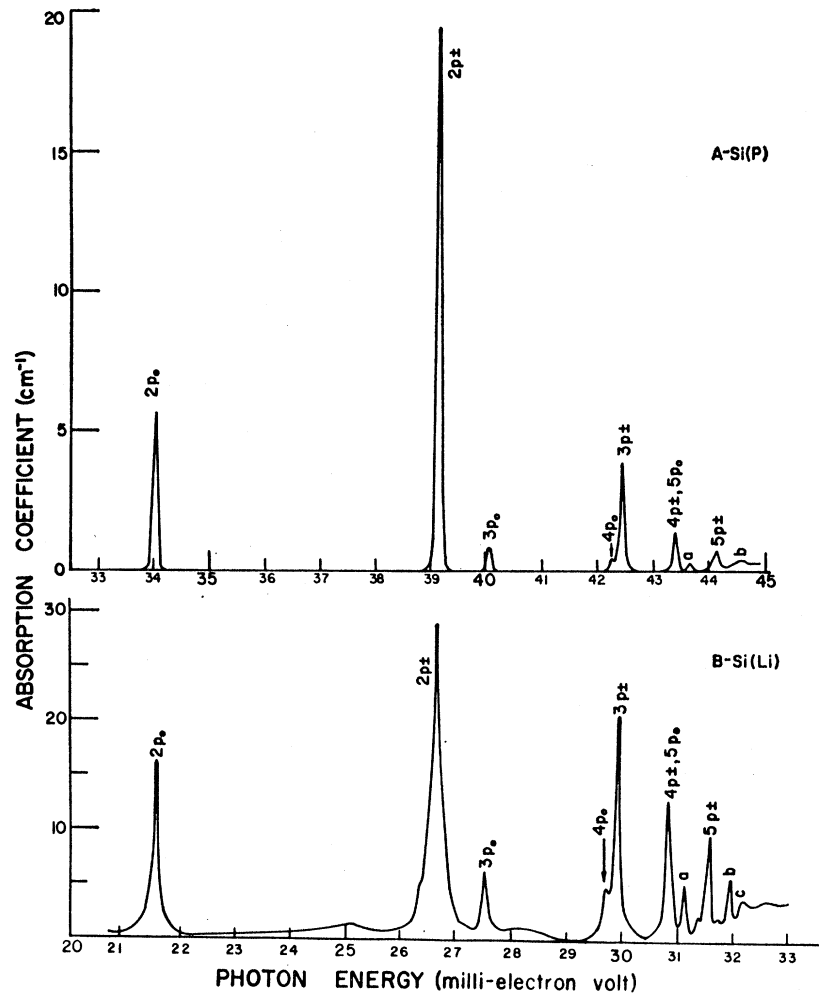
<sup>7</sup> G. Feher, *Phys. Rev.* **114**, 1219 (1959).

<sup>8</sup> R. L. Aggarwal, P. Fisher, V. Mourzine, and A. K. Ramdas, *Bull. Am. Phys. Soc.* **9**, 645 (1964).

<sup>9</sup> In some of the measurements, the short-wavelength contamination was not completely eliminated in the wavelength range  $\sim 45 \mu$  when a grating blazed at  $45 \mu$  was used. Except in the cases when the percent transmission is very low, this does not significantly alter the results.

<sup>10</sup> P. Fisher, W. H. Haak, E. J. Johnson, and A. K. Ramdas, *Proceedings of the Eighth Symposium on the Art of Glassblowing* (The American Scientific Glassblowers Society, Gwinhurst, Wilmington, Delaware, 1963), p. 136.

FIG. 1. (A) The excitation spectrum of phosphorus impurity in silicon;  $N_D \approx 2 \times 10^{14} \text{ cm}^{-3}$ . (B) The excitation spectrum of lithium introduced into high resistivity floating-zone silicon;  $N_D \approx 1 \times 10^{15} \text{ cm}^{-3}$ . Both spectra were measured using liquid-helium coolant. The nature of the excited states giving rise to the lines designated by *a*, *b*, and *c* have not yet been determined.



the polarizer<sup>11</sup> and the technique used for the application of the uniaxial stress have been described elsewhere.<sup>12</sup> Measurements were made using liquid helium and liquid hydrogen as coolants.

### III. EXPERIMENTAL RESULTS

#### A. Excitation Spectra Observed for Zero Stress

##### (i) Lithium in Floating-Zone Silicon

In Fig. 1 is shown the excitation spectrum observed for lithium in floating-zone silicon. The excitation spectrum of phosphorus in silicon is also included in this figure. In Fig. 1 the lines designated by  $2p_0$  in the two spectra have been brought into coincidence; the energy scales for the two spectra are identical. This presentation demonstrates the similarity between the two spectra, viz., the energy spacings between corresponding lines

are the same (see also Table I) while the relative intensities are similar. The energies of the lithium lines are given in Table II.

##### (ii) Lithium in Crucible-Grown Silicon

Lithium introduced into high-resistivity crucible-grown silicon exhibits the excitation spectrum shown

TABLE I. Spacings of excited states for lithium in silicon (in meV).

States	Theory <sup>a</sup>	P <sup>b</sup>	Li <sup>c</sup>	Li-O <sup>d</sup>
$2p_{\pm} - 2p_0$	$5.0 \pm 0.3$	5.06	5.13	5.23
$3p_0 - 2p_{\pm}$	$0.2 \pm 0.7$	0.93	0.88	0.81
$3p_{\pm} - 2p_{\pm}$	$3.0 \pm 0.15$	3.27	3.28	3.18
$4p_0 - 2p_{\pm}$	...	3.11	3.09	3.02 <sup>e</sup>
$4p_{\pm} - 2p_{\pm}$	...	4.21	4.19	4.14
$5p_0 - 2p_{\pm}$	...	4.21	4.19	4.14
$5p_{\pm} - 2p_{\pm}$	...	4.95	4.93	...

<sup>a</sup> See Ref. 6.

<sup>b</sup> See Ref. 12.

<sup>c</sup> The experimental error is  $\pm 0.04$  unit.

<sup>d</sup> The experimental error is  $\pm 0.06$  unit.

<sup>e</sup> Position for the  $1s(A_1) \rightarrow 4p_0$  line of Li-O complex was obtained from the position of the  $4p_0(-)$  line observed in the uniaxial stress measurements for F $\parallel$ [100] (see Fig. 4).

<sup>11</sup> A. Mitsuishi, Y. Yamada, S. Fujita, and H. Yoshinaga, J. Opt. Soc. Am. **50**, 433 (1960).

<sup>12</sup> R. L. Aggarwal and A. K. Ramdas, Phys. Rev. **137**, A602 (1965).

TABLE II. Energies of excitation lines of lithium in silicon (in meV).

Li		
Label	Assignment	Energy
$2p_0$	$1s(E+T_1) \rightarrow 2p_0$	$21.50 \pm 0.02$
$1s(A_1) \rightarrow 2p_{\pm}$	$1s(A_1) \rightarrow 2p_{\pm}$	$24.80 \pm 0.05$
$2p_{\pm}$	$1s(E+T_1) \rightarrow 2p_{\pm}$	$26.63 \pm 0.02$
$3p_0$	$1s(E+T_1) \rightarrow 3p_0$	$27.51 \pm 0.02$
$4p_0$	$1s(E+T_1) \rightarrow 4p_0$	$29.72 \pm 0.02$
$3p_{\pm}$	$1s(E+T_1) \rightarrow 3p_{\pm}$	$29.91 \pm 0.02$
$4p_{\pm}, 5p_0$	$1s(E+T_1) \rightarrow 4p_{\pm}, 5p_0$	$30.82 \pm 0.02$
$a$	?	$31.12 \pm 0.02$
$5p_{\pm}$	$1s(E+T_1) \rightarrow 4p_{\pm}$	$31.56 \pm 0.02$
$b$	?	$31.94 \pm 0.02$
$c$	?	$32.16 \pm 0.02$
Ionization energy <sup>a</sup>		$32.81 \pm 0.06$
Li-O		
Label	Assignment	Energy
$1s(E+T_1) \rightarrow 2p_{\pm}$	$1s(E+T_1) \rightarrow 2p_{\pm}$	$25.60 \pm 0.05$
$x_1$	?	$26.63 \pm 0.02$
$2p_0$	$1s(A_1) \rightarrow 2p_0$	$28.10 \pm 0.03$
$x_2$	?	$29.08 \pm 0.02$
$x_3$	?	$31.86 \pm 0.02$
$x_4$	?	$32.45 \pm 0.03$
$2p_{\pm}$	$1s(A_1) \rightarrow 2p_{\pm}$	$33.33 \pm 0.03$
$3p_0$	$1s(A_1) \rightarrow 3p_0$	$34.14 \pm 0.03$
$4p_0$	$1s(A_1) \rightarrow 4p_0$	$36.35 \pm 0.04$
$3p_{\pm}$	$1s(A_1) \rightarrow 3p_{\pm}$	$36.51 \pm 0.02$
$4p_{\pm}, 5p_0$	$1s(A_1) \rightarrow 4p_{\pm}, 5p_0$	$37.47 \pm 0.03$
Ionization energy <sup>a</sup>		$39.41 \pm 0.07$

<sup>a</sup> The ionization energy has been deduced by adding the theoretically determined binding energy of the  $3p_{\pm}$  state to the experimental energy of the transition labeled  $3p_{\pm}$ .

in Fig. 2. The spectrum of phosphorus in silicon is also included for comparison. Again one finds a spectrum similar to that of a typical Group-V donor. However, there are also lines which do not fit this pattern; these are designated by  $x$ . The spacings of the Group-V-like lines are given in Table I while the energies of all the lines are included in Table II.

### (iii) Lithium in Germanium

In Fig. 3, the excitation spectrum of lithium in germanium is given and is compared with that of arsenic in germanium. The lithium lines occur at positions very close to the excitation lines of arsenic which originate from the excited ground state  $1s(T_1)$ .<sup>13</sup> Table III summarizes the energies of the lines observed for lithium in germanium. It is seen that the lines designated by  $y_1$  and  $y_2$  are absent in the spectrum of arsenic. The intensity of the line  $y_2$  has been found to vary relative to that of the  $1s \rightarrow 2p_{\pm}$  transition, depending upon which technique was employed to introduce lithium. The line at 11.18 meV, has an energy identical to that of the  $1s(A_1) \rightarrow 2p_{\pm}$  line of phosphorus in germanium<sup>13</sup> and is absent for some samples. Thus it is concluded that this arises from a phosphorus contamination.

<sup>13</sup> J. H. Reuszer and P. Fisher, Phys. Rev. **135**, A1125 (1964).

## B. Excitation Spectra Observed Under Uniaxial Stress

Experiments have been performed to examine the effect of uniaxial stress on the lithium excitation spectra of Figs. 1 and 2. Such experiments are useful to determine the assignment of the levels which participate in a given transition, as has been demonstrated for Group-V impurities in both silicon<sup>12</sup> and germanium.<sup>14</sup>

### (i) Lithium in Crucible-Grown Silicon

The effect of a uniaxial compression on the excitation spectrum of lithium in crucible-grown silicon is given in Fig. 4, where  $\mathbf{F}$ , the applied force, is parallel to  $[100]$ . The upper curve represents results for the electric vector  $\mathbf{E} \parallel \mathbf{F}$  and the lower for  $\mathbf{E} \perp \mathbf{F}$ . The dashed curve in each case is for  $\mathbf{F} = 0$ . The results of a similar measurement for phosphorus in silicon are shown in Fig. 5. The latter is included for purposes of comparison.

### (ii) Lithium in Floating-Zone Silicon

The spectrum of lithium in floating-zone silicon under uniaxial compression along  $[100]$  and  $[110]$  are shown in Figs. 6–8. In Figs. 7 and 8 the direction of light propagation  $\mathbf{q}$  is along  $[1\bar{1}0]$  and  $[001]$ , respectively. The results for  $\mathbf{F} \parallel [111]$  are presented in Fig. 9. Due to experimental limitations, the measurements for  $\mathbf{E} \parallel \mathbf{F}$ , in Fig. 9, do not extend to the lower energies.

## IV. DISCUSSION

### (i) Lithium in Crucible-Grown Silicon

The results given in Fig. 2 and Table I strongly suggest that the excitation lines (with the exception of the  $x$  lines) are due to transitions to excited states which are identical to those of the Group-V impurities. Hence, the excitation lines of Fig. 2 have been labeled accordingly. The actual spectral region in which the spectrum occurs is governed by the chemical splitting and shift

TABLE III. Energies of excitation lines of lithium in germanium (in meV).

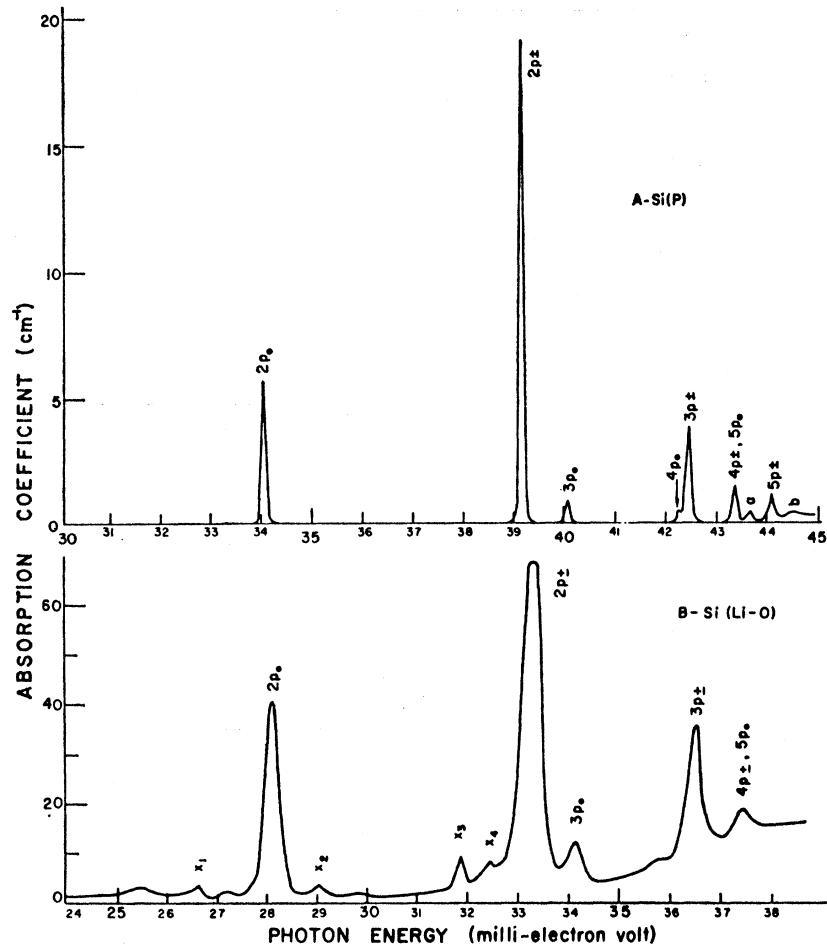
Label	Energy
$1s \rightarrow 2p_0$	$5.25 \pm 0.02$
$1s \rightarrow 3p_0$	$7.45 \pm 0.03$
$y_1$	$7.68 \pm 0.03$
$1s \rightarrow 2p_{\pm}$	$8.29 \pm 0.02$
$y_2$	$8.72 \pm 0.02$
$1s \rightarrow 3p_{\pm}$	$8.96 \pm 0.02$
$1s \rightarrow ?$	$9.29 \pm 0.03$
	$9.45 \pm 0.03$
$1s \rightarrow \text{C.B.}^a$	$9.89 \pm 0.05$
Ionization energy <sup>b</sup>	
	$9.89 \pm 0.05$

<sup>a</sup> C.B. denotes conduction band.

<sup>b</sup> This energy was estimated using the binding energy of the  $2p_{\pm}$  state and the energy of the transition  $1s \rightarrow 2p_{\pm}$ .

<sup>14</sup> J. H. Reuszer and P. Fisher, Bull. Am. Phys. Soc. **9**, 645 (1964).

FIG. 2. (A) See Fig. 1(A). (B) The excitation spectrum of lithium introduced into  $\sim 150 \Omega\text{-cm}$   $p$ -type crucible-grown silicon, with oxygen concentration of  $\sim 5 \times 10^{17} \text{ cm}^{-3}$ ;  $N_D \approx 6 \times 10^{18} \text{ cm}^{-3}$ . Measurement was made with liquid-helium coolant.



of the ground state.<sup>13,15</sup> The spectra exhibited by lithium in floating-zone and crucible-grown silicon are observed in different spectral regions. Further, the two spectra have not been observed for the same sample. Floating-zone silicon and crucible-grown silicon differ from one another in the amount of oxygen each contains.<sup>16</sup> As judged from the  $9\text{-}\mu$  vibrational band, the latter has typically  $5 \times 10^{17}$  oxygen atoms per cc whereas the former exhibits no  $9\text{-}\mu$  band, giving an upper limit of  $\sim 10^{16}$  oxygen atoms per cc for the floating-zone material. Lithium is known to form donor complexes with oxygen.<sup>3</sup> We attribute the excitation spectrum observed in crucible-grown silicon to these lithium-oxygen (Li-O) complexes<sup>17</sup> and the spectrum observed in floating-zone silicon to isolated lithium. The rather large half-width of the excitation lines for the Li-O complex as compared to that for phosphorus is an interesting feature of the spectrum.

<sup>15</sup> R. L. Aggarwal, *Solid State Commun.* **2**, 163 (1964).

<sup>16</sup> W. Kaiser, P. H. Keck, and C. F. Lange, *Phys. Rev.* **101**, 1264 (1956). See also W. Kaiser and P. H. Keck, *J. Appl. Phys.* **28**, 882 (1957).

<sup>17</sup> The electronic excitation spectrum of oxygen "decorated" by lithium appears to offer a more sensitive means for the determination of the oxygen concentration in silicon than the  $9\text{-}\mu$  vibrational band.

The stress effects for the Li-O complex for  $\mathbf{F} \parallel [100]$  shown in Fig. 4, exhibit the following features: (1) The excitation lines labeled  $2p_0$ ,  $2p_{\pm}$ ,  $3p_{\pm}$  clearly split into two components, one to the low-energy side and the other to the high-energy side of the zero-stress position. All the doublets have the same spacing. Also, they are identically disposed about their respective zero-stress positions, although not symmetrically. (2) The high-energy component of the  $2p_0$  line appears for  $\mathbf{E} \perp \mathbf{F}$  whereas the low-energy component appears for  $\mathbf{E} \parallel \mathbf{F}$ . On the other hand, both components of the  $2p_{\pm}$  and  $3p_{\pm}$  lines appear for  $\mathbf{E} \perp \mathbf{F}$  and only the high-energy components for  $\mathbf{E} \parallel \mathbf{F}$ . A comparison of Figs. 4 and 5 shows that the behavior of the lines of the Li-O complex under stress is identical to the behavior of their counterparts in the phosphorus spectrum. The behavior of the remaining Group-V-like lines for the Li-O complex is consistent with the behavior of the corresponding lines in the phosphorus spectrum. The stress effects for phosphorus have been explained<sup>12</sup> in the framework of the effective mass and the deformation potential theories. The two components which each line exhibits are due to transitions from the singlet  $1s(A_1)$  state to an excited  $p$  state which has split into

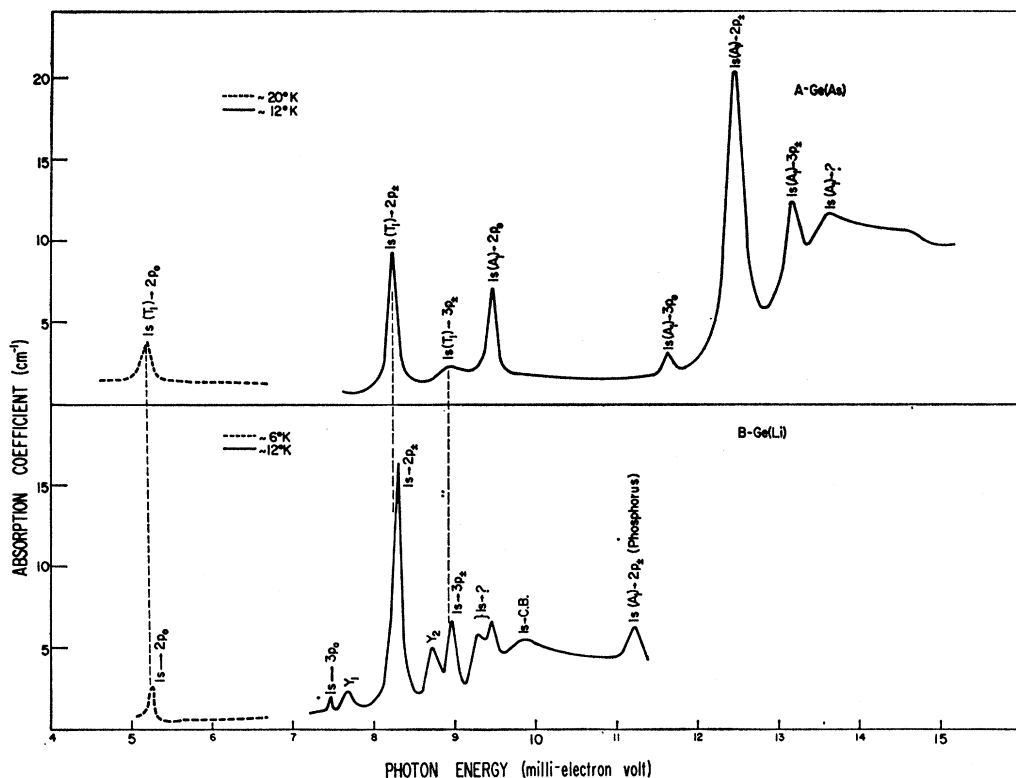


FIG. 3. (A) The excitation spectrum of arsenic in germanium;  $N_D \approx 1 \times 10^{15} \text{ cm}^{-3}$ . (B) The excitation spectrum of lithium in germanium. Lithium was introduced into the germanium in the melt;  $N_D \approx 2 \times 10^{14} \text{ cm}^{-3}$ .

two states under the uniaxial stress. The detailed similarity of the stress-induced behavior of the Li-O complex and phosphorus implies that the site symmetry of the former is  $T_d$  (in the absence of stress) and that the lowest ground state of the Li-O complex is a  $1s(A_1)$  state.

The lines denoted by  $x$  in Fig. 4 also exhibit splittings and dichroic effects. These features for the line  $x_3$  suggest that it is due to a transition to a  $p_{\pm}$  level. The results for lines  $x_1$ ,  $x_2$ , and  $x_4$  are not conclusive since the intensities are very small.

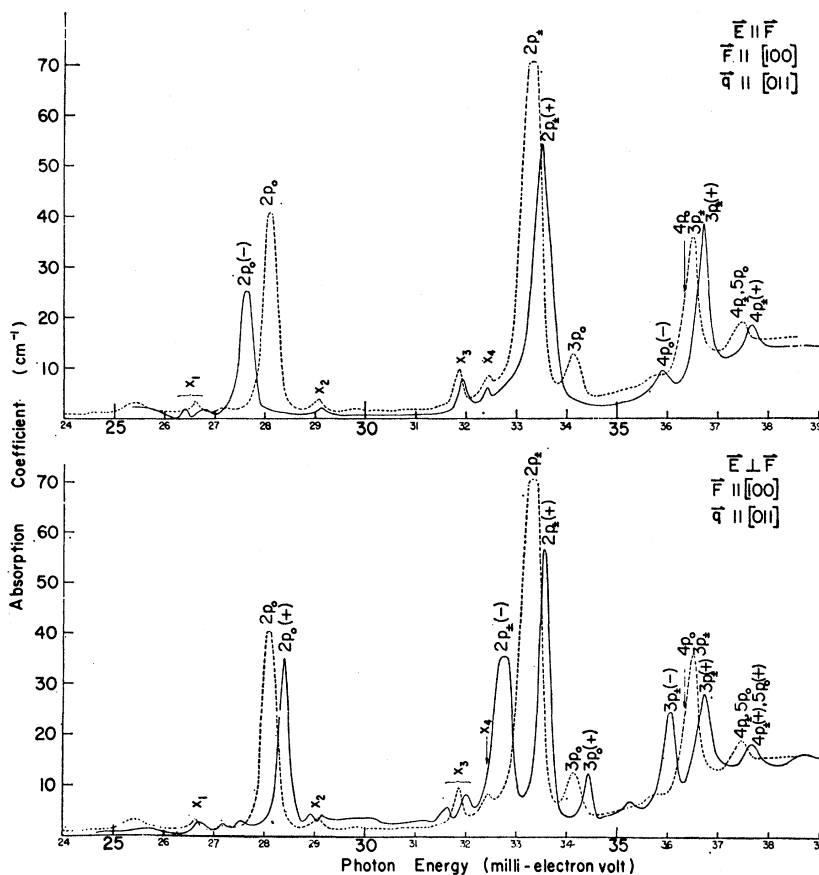
In view of the close similarity between the energy level schemes of the Li-O complex and phosphorus, it is expected that the Li-O donor will also have higher lying  $1s$  states. Experiments have been performed at higher temperatures to observe transitions from these states to the  $p$  states. These results are shown in Fig. 10 for liquid-hydrogen temperature. A peak is observed at 25.6 meV which is  $7.7 \pm 0.1$  meV to the low-energy side of the transition  $1s(A_1) \rightarrow 2p_{\pm}$ . If this is interpreted as a transition from the  $1s(E) + 1s(T_1)$  levels (assumed to be degenerate) to the  $2p_{\pm}$  level, then the chemical splitting is 7.7 meV which is consistent with the spectral range in which the transitions from  $1s(A_1)$  occur. In the case of the Group-V impurities,<sup>15</sup> the  $1s(E)$  and  $1s(T_1)$  states are energetically separated; this does not appear to be so for the Li-O complex.

Indeed this separation does vary from impurity to impurity (1.35 meV for phosphorus to 2.5 meV for antimony). The transition from  $1s(E) + 1s(T_1)$  to the  $2p_0$  level was not observed; this line is expected to be weaker than the corresponding transition to the  $2p_{\pm}$  state.

#### (ii) Lithium in Floating-Zone Silicon

From the results of Fig. 1, it is quite clear that the excitation lines for isolated lithium are due to transitions to excited  $p$  states which are identical to those of phosphorus. From a comparison of the spectral regions in which the excitations for isolated lithium and phosphorus occur, it is concluded that the chemical splitting for isolated lithium is very small. If the chemical splitting for isolated lithium is practically zero, it is clear from Fig. 11 that the excitation lines will not split under the application of uniaxial stress. This is not borne out experimentally (see Figs. 6-8). Instead, it is seen that each line splits into three components; a component to the low-energy side of the zero-stress position, a component to the high-energy side of the zero-stress position and a component coincident with the zero-stress position. If it is assumed that the isolated lithium occupies the tetrahedral interstitial site and that the level structure of the ground state is similar to that of the Group-V impurities, i.e., the lowest level

FIG. 4. The effect of a  $[100]$  compression on the excitation spectrum of Fig. 2(B) for  $\mathbf{q} \parallel [011]$ . The upper curve is for  $\mathbf{E} \parallel \mathbf{F}$  and the lower is for  $\mathbf{E} \perp \mathbf{F}$ . The dashed curve in each diagram is for  $\mathbf{F} = 0$ .



is the singlet  $1s(A_1)$ , then the stress induced spectrum should have been similar to that exhibited by phosphorus. This is not the case.

If, instead, it is assumed that the  $1s(A_1)$  state lies above the  $1s(E+T_1)$  state, i.e., the chemical splitting is opposite to that of the Group-V impurities, then the stress effects shown in Fig. 12 obtain for uniaxial compression along  $[100]$ . The level scheme has been deduced using the perturbation calculation given by Price<sup>18</sup> and Wilson and Feher,<sup>19</sup> with  $\delta\Delta_e$ , the chemical splitting, however, assumed to be of opposite sign to that of Ref. 19 (see the Appendix). The excited  $p$  states under stress will, of course, behave identically to those of the Group-V impurities; this is also shown in Fig. 12. The selection rules given in this figure were deduced using matrix elements of the type given by Kohn in Ref. 6, Sec. 5c. This energy level scheme permits a transition not only of the same energy as the zero-stress transition, but also a transition of a higher and of a lower energy. These conclusions, along with the predictions regarding the polarization behavior of the components, are in excellent agreement with the experimental results given in Fig. 6.

With the above choice of ground-state structure, the

case of  $\mathbf{F} \parallel [110]$  is now considered. For this direction of stress, the site symmetry of the interstitial lithium changes from  $T_d$  to that of  $C_{2v}$ .<sup>12</sup> The orthorhombic axes of this point group are  $[110]$ ,  $[\bar{1}\bar{1}0]$ , and  $[001]$ . In this case, the selection rules for polarized light depend upon the direction of light propagation  $\mathbf{q}$  as is shown in Fig. 13 for  $\mathbf{q} \parallel [1\bar{1}0]$  and  $[001]$ . A comparison of the results given in Figs. 7 and 8 with the predictions of Fig. 13 clearly demonstrates that the experimental observations are in agreement with the above model for the ground states.

The excitation spectrum with  $\mathbf{F} \parallel [111]$ , Fig. 9, shows no splittings as is to be expected in the framework of the effective-mass approximation and the deformation potential theory.<sup>12</sup> Attention should be drawn here to the dichroism displayed by the spectrum.

From the spacings of the stress-induced components of the excitation lines and the splitting of the excited states<sup>20</sup> for uniaxial stress along the  $[100]$  or the  $[110]$  direction, an estimate of  $\delta\Delta_e$  has been made. This is

<sup>20</sup> Of the samples examined under stress, some were prepared by diffusing lithium into phosphorus-doped floating-zone silicon. The behavior of the phosphorus  $2p_{\pm}$  line under stress gave a direct measure of the splitting of the excited states of the lithium impurity. Within the experimental error, the spacing between the low- and the high-energy components of the lithium lines, under stress, is equal to the energy difference of the  $2p_{\pm}(+)$  and  $2p_{\pm}(-)$  lines of the phosphorus.

<sup>18</sup> P. J. Price, Phys. Rev. **104**, 1223 (1956).

<sup>19</sup> D. K. Wilson and G. Feher, Phys. Rev. **124**, 1068 (1961).

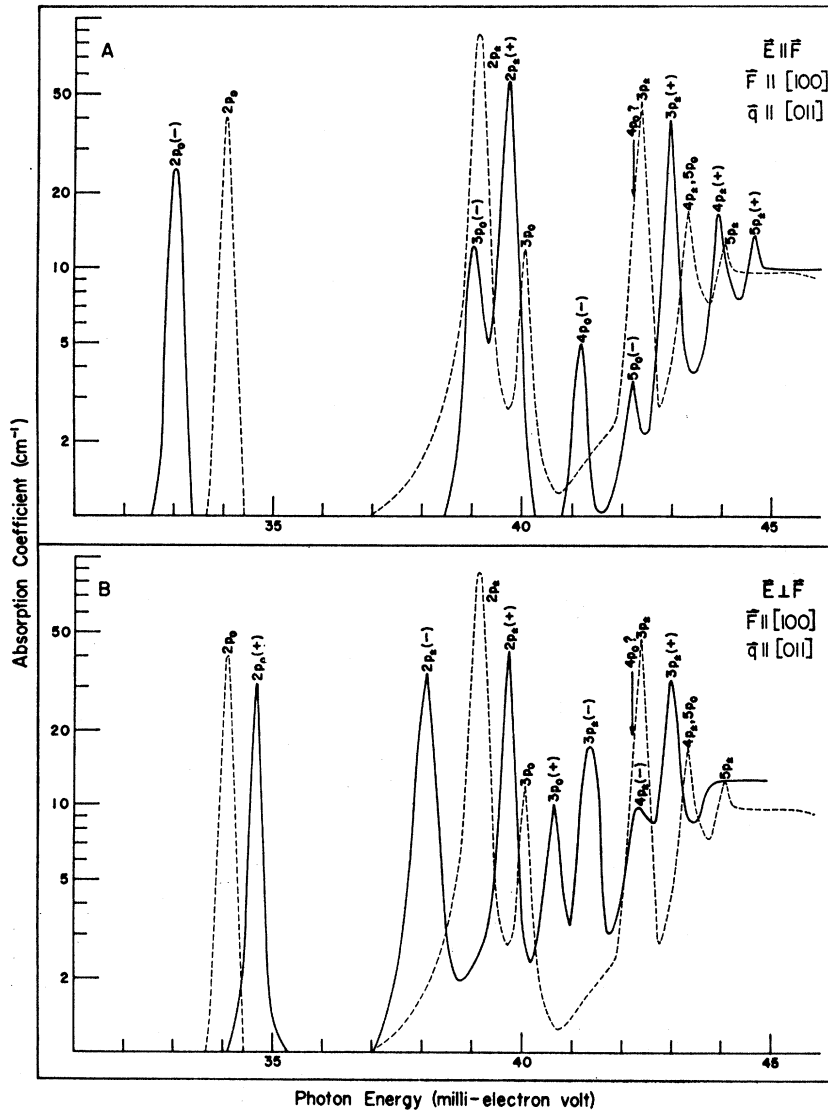


FIG. 5. The effect of a [100] compression on the excitation spectrum of phosphorus in silicon;  $N_D \approx 4 \times 10^{15} \text{ cm}^{-3}$ . The upper curve is for  $E \parallel F$  and the lower is for  $E \perp F$ . The dashed curves are for  $F=0$ .

found to be  $1.6 \pm 1 \text{ meV}$ , the error being a statistical one based on the results of ten measurements. For this value of  $6\Delta_e$ , the  $1s(A_1)$  state should be sufficiently populated at liquid-hydrogen temperature such that transitions from this state to the  $p$  states should be observable. Experiments have been performed at this temperature; the results are given in Fig. 14. A relatively broad absorption line,  $1.8 \pm 0.1 \text{ meV}$  to the low-energy side of the transition labeled  $2p_{\pm}$ , is clearly seen at this temperature. This line is interpreted as being due to the transition  $1s(A_1) \rightarrow 2p_{\pm}$ . Experiments have also been performed under uniaxial compression along [100] at liquid-hydrogen temperature; these results are included in Fig. 14. It is seen that the line designated by  $1s(A_1) \rightarrow 2p_{\pm}$  splits into a low-energy and a high-energy component. No component is observed at the zero-stress position. This behavior is identical to that

of the  $1s(A_1) \rightarrow 2p_{\pm}$  transition of phosphorus in silicon, as can be seen in the figure. This further supports the interpretation that this transition arises from the  $1s(A_1)$  state. The  $1s(A_1) \rightarrow 2p_0$  transition was not observed. However, it is expected to be weak.

### (iii) Lithium in Germanium

The spectrum of lithium in germanium exhibits some lines which are close to the energies of the transitions from  $1s(T_1)$  to the excited  $p$  states of the Group-V impurities (see Fig. 3), i.e., these lines have energies which are close to those predicted by the effective-mass theory. Since this spectrum has yet to be examined under uniaxial stress, it cannot be concluded whether the ground state has no chemical splitting or whether it has the "inverted" ground-state structure which appears to be the case for lithium in silicon.

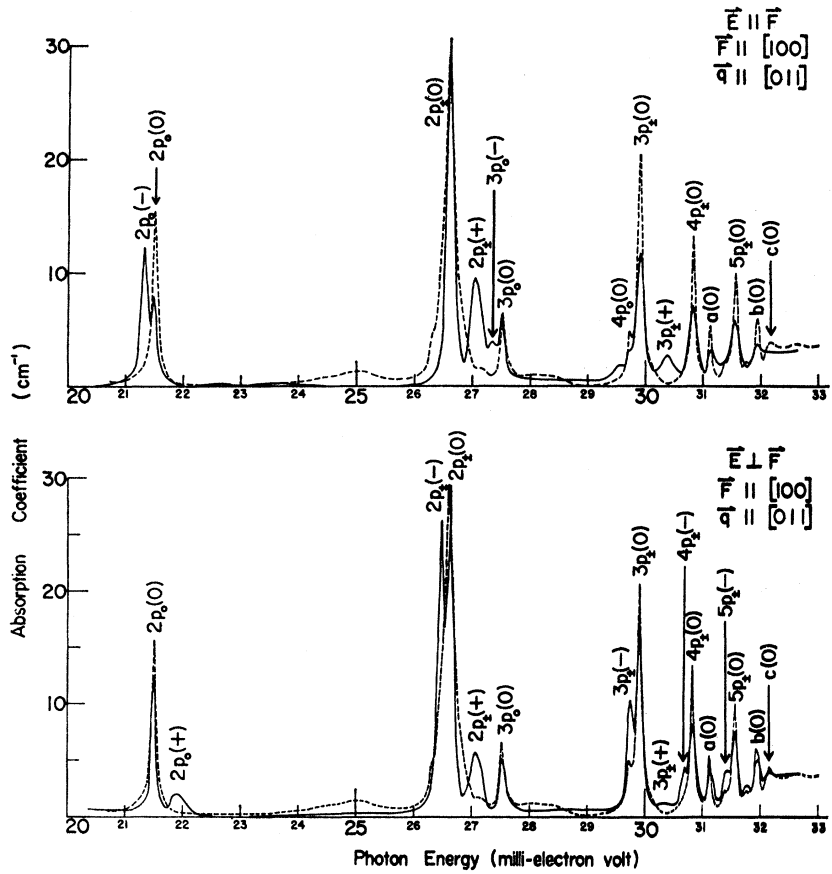


FIG. 6. The effect of a [100] compression on the excitation spectrum of Fig. 1(B) for  $q \parallel [011]$ . The upper curves for  $E \parallel F$  and the lower for  $E \perp F$ . The dashed curves are for  $F=0$ .

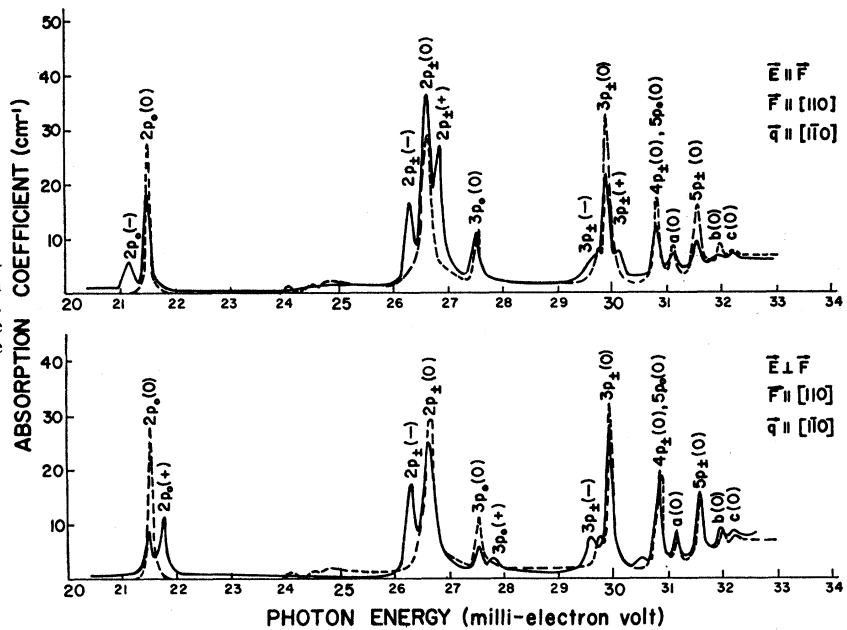


FIG. 7. The effect of a [110] compression on the excitation spectrum of lithium in silicon for  $q \parallel [110]$ ;  $N_D \approx 1 \times 10^{16} \text{ cm}^{-3}$ . The upper curve is for  $E \parallel F$  and the lower for  $E \perp F$ . The dashed curves are for  $F=0$ .

V. CONCLUSIONS

The excitation spectra of lithium and lithium-oxygen complex observed in the present investigation have been

interpreted in the framework of the effective-mass theory, assuming a  $T_d$  site symmetry for the donors. This model is consistent with all the present observations.

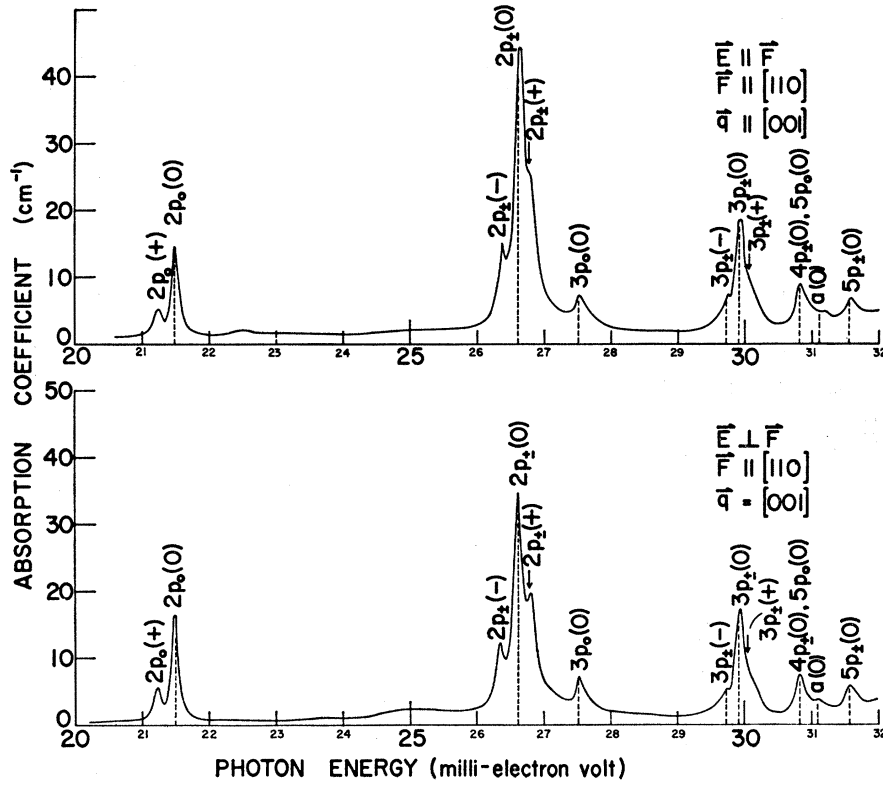


FIG. 8. The effect of a  $[110]$  compression on the excitation spectrum of lithium in silicon for  $q \parallel [001]$ ;  $N_D \approx 1 \times 10^{15} \text{ cm}^{-3}$ . The upper curve is for  $E \parallel F$  and the lower for  $E \perp F$ . The vertical dashed lines indicate the positions of the excitation lines for  $F=0$ .

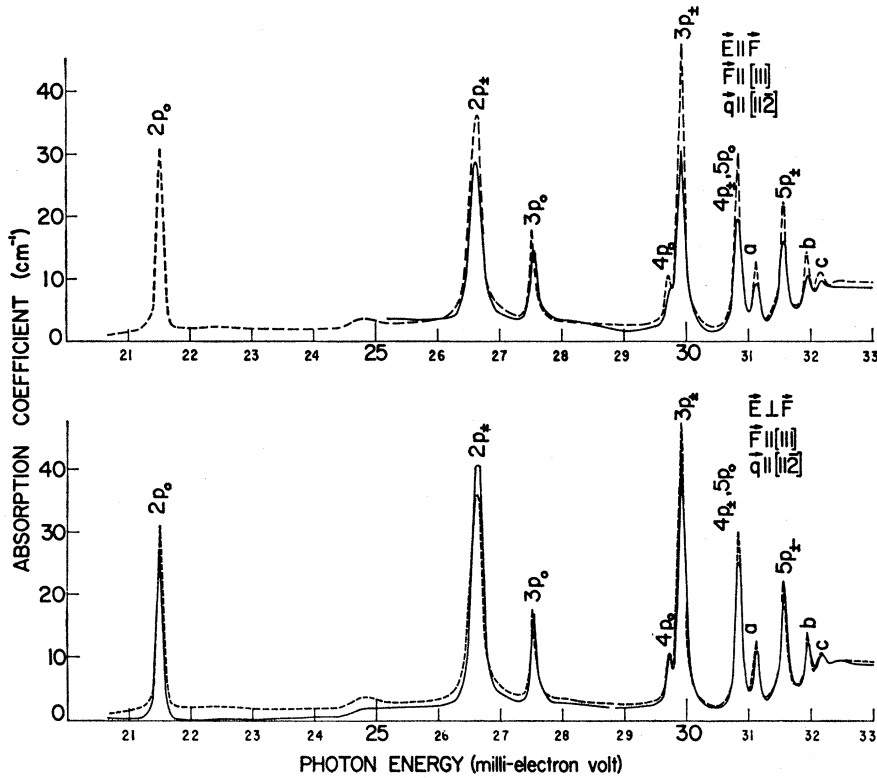


FIG. 9. The effect of a  $[111]$  compression on the excitation spectrum of lithium in silicon for  $q \parallel [112]$ ;  $N_D \approx 2 \times 10^{15} \text{ cm}^{-3}$ . The upper curve is for  $E \parallel F$  and the lower for  $E \perp F$ . The dashed curves are for  $F=0$ .

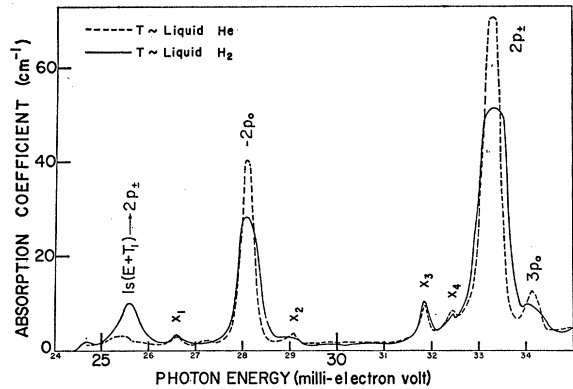


FIG. 10. The excitation spectrum of lithium-oxygen complex in silicon at liquid-helium and liquid-hydrogen temperatures. The sample used was the same as that of Fig. 2.

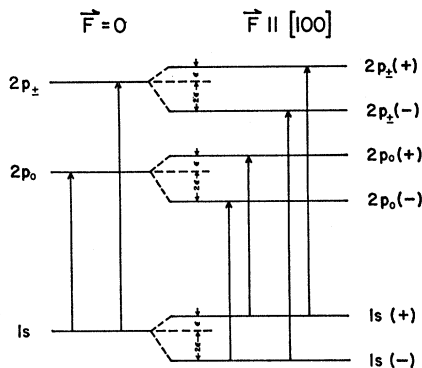


FIG. 11. Splitting of the donor levels in silicon under a [100] compression for  $6\Delta_c=0$  (not to scale). The allowed transitions are shown by the vertical arrows. For a definition of  $\epsilon$ , see the Appendix.

It has been suggested by Weiser,<sup>4</sup> on the basis of the mechanism for diffusion of lithium in the diamond-type lattice, that the site symmetry of isolated lithium is not

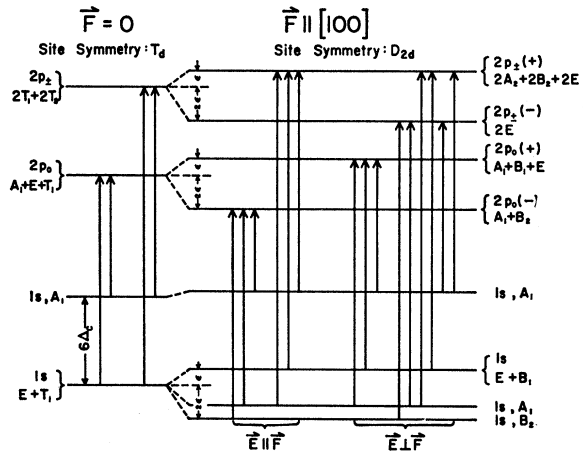


FIG. 12. Splitting of the donor levels in silicon (not to scale) under a [100] compression for a finite  $6\Delta_c$  and with an "inverted" Group-V-like ground state. The vertical arrows indicate the allowed transitions. The capital letters labeling the levels denote the irreducible representations of  $T_d$  and  $D_{2d}$  to which the states belong. For a definition of  $\epsilon$ , see the Appendix.

tetrahedral but hexagonal. The observed features of the spectra in the present investigation find a satisfactory explanation for all the cases assuming a tetrahedral site symmetry. It is felt that it would be fortuitous for lithium in the hexagonal site to give a spectrum identical, in all its details, to that when it occupies the tetrahedral site. Feher<sup>7</sup> did not observe a spin resonance in lithium-doped floating-zone silicon, i.e., for isolated lithium. This is not surprising if the ground-state energy scheme proposed in the present paper is correct, i.e., a ground state with a high degree of degeneracy. For example, it is well known that for acceptors in silicon, because of the degeneracy of the ground states, the spin resonance is broadened beyond detection by strain in-

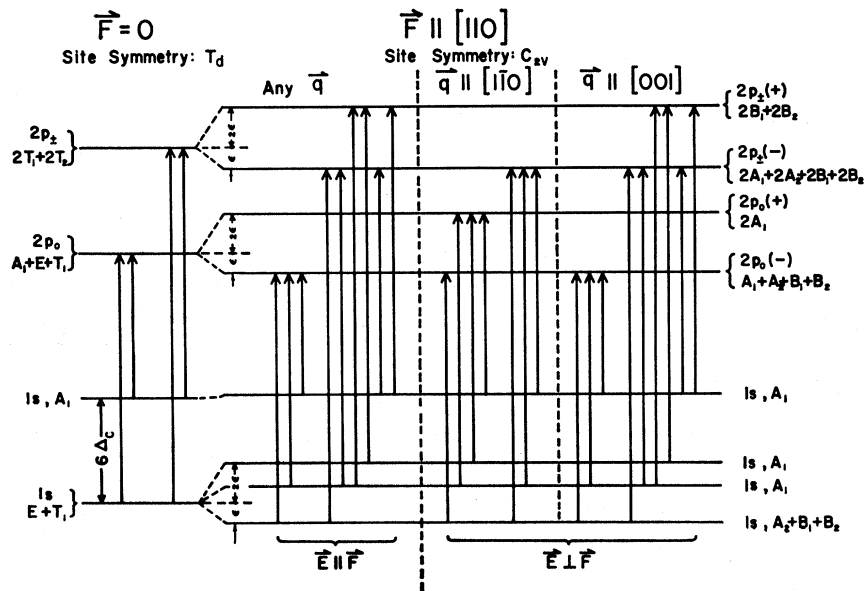


FIG. 13. Splitting of the donor levels of Fig. 12 under a [110] compression. The allowed transitions are shown for  $q \parallel [110]$  and  $q \parallel [001]$ . Here  $3\epsilon$  is the energy difference between the valleys along [100],  $[1\bar{1}0]$ ,  $[010]$ , and  $[0\bar{1}0]$  on the one hand, and those along  $[001]$  and  $[00\bar{1}]$  on the other hand.

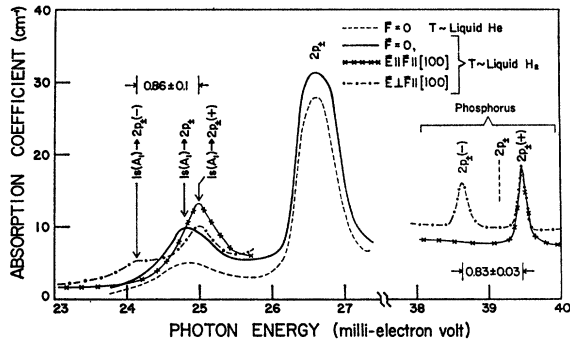


FIG. 14. Part of the excitation spectrum of isolated lithium in phosphorus-doped silicon.  $N_D \approx 4 \times 10^{15} \text{ cm}^{-3}$ . (a) Liquid-helium temperature,  $F=0$  (dashed line); (b) liquid-hydrogen temperature,  $F=0$  (solid line); (c) liquid-hydrogen temperature,  $E||F||[100]$  (line on left with crosses); (d) same as (c) but with  $E\perp F$  (dot-dash line on left); (e) and (f) the  $2p_{\pm}$  line of phosphorus for  $E||F$  and  $E\perp F$ , respectively (corresponding lines on right). Curves (c) to (f) were obtained during the same measurement.

homogeneities normally present in the material.<sup>6,21</sup> For these centers, when the degeneracy of the ground state is removed by a uniaxial stress, sharp resonances have been observed. This appears also to be the case for isolated lithium in silicon, since Watkins<sup>22</sup> has observed sharp electron spin resonances under uniaxial stress for samples identical to those used in the present investigation.

The small magnitude of the chemical splitting for the isolated lithium may be accounted for in a qualitative manner. It is reasonable to expect that isolated interstitial lithium will produce considerably less deformation of the lattice than the substitutional Group-V impurities, and hence, the contribution to the chemical splitting due to this effect should be small for isolated lithium. On the same basis, the larger chemical splitting for the Li-O complex may also be understood.

The present results for the lithium-oxygen complex indicate that it has a tetrahedral symmetry and that its ground state is the singlet  $1s(A_1)$ . Feher<sup>7</sup> did observe electron spin resonance for such complexes without uniaxial stress which appears to confirm that the ground state is a singlet. However, a small anisotropy in the  $g$  factor was observed by him, from which he concludes that the spin-resonance center involved does not have tetrahedral symmetry. It is not clear to what extent the lithium-oxygen complex must depart from tetrahedral symmetry before the optical spectra give evidence for this.

In conclusion, attention should be drawn to the thermal activation energy given by Morin *et al.*<sup>5</sup> for lithium in silicon. This value, 33 meV, is in excellent agreement with the present optical activation energy for lithium in oxygen-free silicon. This agreement is rather surprising as the samples used by Morin *et al.*

<sup>21</sup> G. Feher, J. C. Hensel, and E. A. Gere, Phys. Rev. Letters 5, 309 (1960).

<sup>22</sup> G. D. Watkins (private communication).

were almost certainly oxygen-containing and thus the activation energy should have been closer to 39.41 meV, the activation energy obtained in the present work for the Li-O complex.

#### ACKNOWLEDGMENTS

We wish to thank Miss Louise Roth for the preparation of the germanium crystals and for orienting the samples used in the stress measurements. We also wish to thank Dr. G. D. Watkins, of the General Electric Laboratory, for useful discussions and for communicating to us the results of his spin-resonance experiments on lithium in silicon prior to publication.

#### APPENDIX

In this section an analysis is given to determine the behavior in silicon of an "inverted" Group-V-like ground state under uniaxial stress. Following Price<sup>18</sup> and Wilson and Feher,<sup>19</sup> the energies of the ground states under a uniaxial stress along  $[100]$  are given by the solution of the following secular equation:

$$\begin{vmatrix} -2\epsilon - E & \Delta_c & \Delta_c & \Delta_c & \Delta_c & \Delta_c \\ \Delta_c & -2\epsilon - E & \Delta_c & \Delta_c & \Delta_c & \Delta_c \\ \Delta_c & \Delta_c & \epsilon - E & \Delta_c & \Delta_c & \Delta_c \\ \Delta_c & \Delta_c & \Delta_c & \epsilon - E & \Delta_c & \Delta_c \\ \Delta_c & \Delta_c & \Delta_c & \Delta_c & \epsilon - E & \Delta_c \\ \Delta_c & \Delta_c & \Delta_c & \Delta_c & \Delta_c & \epsilon - E \end{vmatrix} = 0,$$

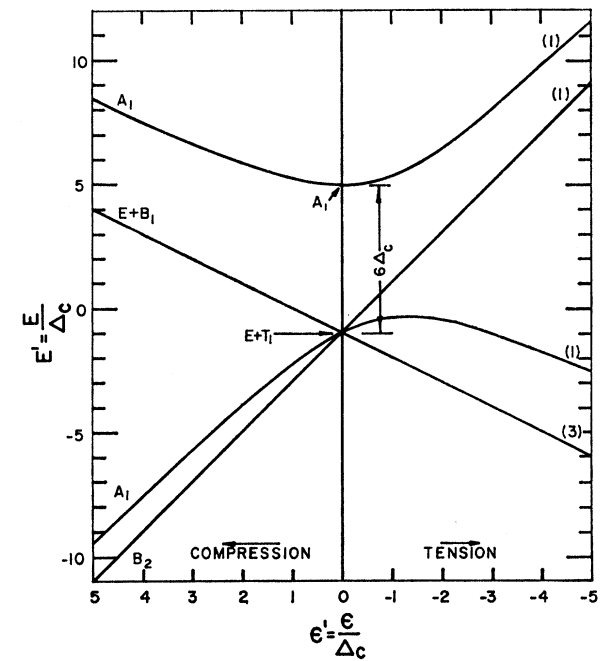


FIG. 15. Splitting of an "inverted" Group-V-like ground state of a donor in silicon under strain for  $F||[100]$ .  $E' = E/\Delta_c$  and  $\epsilon' = \epsilon/\Delta_c$  where  $E$  is the energy of a given state and  $3\epsilon$  is the energy difference between the  $\langle 100 \rangle$  conduction-band minima. The numbers in parentheses indicate the degeneracies of the various states while the letters denote the relevant irreducible representations of  $D_{2d}$ , the site symmetry for this direction of stress.

where

$$\epsilon = -\frac{1}{3}\Xi_u(S_{11}-S_{12})T; \quad S_{11} \text{ and } S_{12},$$

are the elastic compliance constants,  $T$  is the applied stress and  $\Xi_u$  is the shear-deformation-potential constant of the conduction-band minima. Also,  $6\Delta_c$  = chemical splitting of the ground state. The  $1s(E)$  and  $1s(T_1)$  states are assumed to be degenerate. The solutions to the secular equation are

$$\epsilon - \Delta_c \text{ (3 roots), } -2\epsilon - \Delta_c, \text{ and } \\ \frac{1}{2}[(4\Delta_c - \epsilon) \pm (9\epsilon^2 + 12\epsilon\Delta_c + 36\Delta_c^2)^{1/2}].$$

The variation of the ground states with strain is shown in Fig. 15. It is seen that the two states described by the first two types of roots vary with strain in a manner which is identical to that of the  $p$  states.

The following linear combinations of the effective-mass wave functions permit the selection rules of Fig. 12 to be deduced

$$\alpha_j^{(1)}: \quad 2^{-1/2}(1, -1, 0, 0, 0, 0) \quad (B_2), \\ \alpha_j^{(2)}: \quad (a, a, b, b, b, b) \quad (A_1),$$

$$\alpha_j^{(3)}: \quad \frac{1}{2}(0, 0, 1, 1, -1, -1) \quad (B_1), \\ \alpha_j^{(4)}: \quad 2^{-1/2}(0, 0, 1, -1, 0, 0) \\ \alpha_j^{(5)}: \quad 2^{-1/2}(0, 0, 0, 0, 1, -1) \\ \alpha_j^{(6)}: \quad (c, c, d, d, d, d) \quad (A_1),$$

where, for  $\chi_j = F_j \varphi_j$  (see Ref. 6), the corresponding wave functions are

$$\psi^{(i)} = \sum_{j=1}^6 \alpha_j^{(i)} \chi_j,$$

and the valleys labeled  $j=1, \dots, 6$ , have their major axes along  $[100]$ ,  $[\bar{1}00]$ ,  $[010]$ ,  $[0\bar{1}0]$ ,  $[001]$ , and  $[00\bar{1}]$ , respectively;

$$a^2 = \frac{1}{4}(1+\beta), \quad b^2 = \frac{1}{8}(1-\beta), \quad c^2 = \frac{1}{4}(1-\beta) \quad \text{and} \quad d^2 = \frac{1}{8}(1+\beta)$$

and

$$\beta = (3\epsilon + 2\Delta_c)(9\epsilon^2 + 12\epsilon\Delta_c + 36\Delta_c^2)^{-1/2}.$$

The letters in parentheses refer to the irreducible representations of  $D_{2d}$ , the point group symmetry of the impurity for  $\mathbf{F} \parallel [100]$ .

## Color Centers Produced in KCl and KBr by Prolonged X Irradiations at Low Temperatures

BRUCE J. FARADAY\* AND W. DALE COMPTON†

*U. S. Naval Research Laboratory, Washington, D. C.*

(Received 5 November 1964)

The principal purposes of this study were to observe the effect of an x irradiation of extended duration on the production of color centers in KCl and KBr at low temperatures and to examine the implications with regard to possible color-center models. Growth curves were determined at 5°K for the  $F$ ,  $K$ ,  $M$ , and  $H$  bands in KCl and KBr and for a new band at 245  $m\mu$  in KCl and at 278  $m\mu$  in KBr, called the  $H'$  band. Growth curves were determined at 80°K for the  $F$ ,  $K$ , and  $M$  bands in KCl and KBr. The growth of the  $V_4$  band in KBr and of a band having its absorption maximum at 240  $m\mu$  in KCl, designated as the  $V(240)$  band, was also followed at 80°K. The ratio of the absorptions at the peak of the  $F$  and  $K$  bands was found to remain constant indicating that both of these bands arise from transitions in the same center. The concentration of  $M$  centers was found to depend quadratically on the  $F$ -center concentration. This result gives conclusive support to the model proposed by van Doorn and Haven that the  $M$  center consists of a pair of associated  $F$  centers. The  $F$ -to- $H$  ratio was observed to be constant for short x-ray exposures, supporting the viewpoint that the two centers are produced as complementary defects; however, for prolonged exposures, this ratio is no longer constant. The number of  $F$  centers is in constant ratio to the combined concentrations of  $H$  and  $H'$  centers provided that the oscillator strength of the  $H'$  band is suitably chosen. The linear dependence of the generation of both  $V_4$  centers in KBr and  $V(240)$  centers in KCl on  $F$ -center concentration suggests that the  $V_4$  and  $V(240)$  centers, rather than  $V_1$  centers, are fundamentally related to the mechanism of formation of  $F$  centers near liquid-nitrogen temperature for a prolonged irradiation.

### I. INTRODUCTION

IT is well known that the types of color centers produced by ionizing radiation and the concentrations of each are very much dependent on the temperature

of irradiation. Accordingly, a considerable effort has been expended in studying the role of temperature in the formation of radiation-induced defects in the alkali halides. The major part of this research has been confined to three principal temperature regions, conveniently defined, as follows: the liquid-helium temperature range (at 5°K), the liquid-nitrogen range (at 80°K) and room temperature (295° to 300°K). The principal

\* A portion of this work was submitted to the faculty of the Catholic University of America in partial fulfillment of the requirements for the degree of Doctor of Philosophy.

† Present address: Department of Physics, University of Illinois, Urbana, Illinois.